Title
Seismic soil-structure interaction in buildings. II: Empirical findings

Journal
J. Geotech. & Geoenv. Engrg., 125(1)

Authors
Stewart, Jonathan P
Seed, Raymond B
Fenves, Greggory L

Publication Date
1999

Peer reviewed

SEISMIC SOIL-STRUCTURE INTERACTION IN BUILDINGS. II: EMPIRICAL FINDINGS

By Jonathan P. Stewart,[1] Raymond B. Seed,[2] and Gregory L. Fenves,[3] Members, ASCE

ABSTRACT: System identification analyses are used to evaluate soil-structure interaction effects for 77 strong motion data sets at 57 building sites that encompass a wide range of structural and geotechnical conditions. Kinematic interaction effects on the ''input'' motion at the bases of structures are found to be relatively modest in many cases, whereas inertial interaction effects on the structural response to these motions can be significant. To quantify inertial interaction effects, fixed- and flexible-base modal vibration parameters are used to evaluate first-mode period lengthening ratios $\tilde{T}/T$ and foundation damping factors $\tilde{\zeta}_0$. The response of some structures is dominated by inertial interaction (e.g., $\tilde{T}/T \approx 4$, $\tilde{\zeta}_0 \approx 30\%$), whereas others undergo negligible soil-structure interaction (e.g., $\tilde{T}/T \approx 1$, $\tilde{\zeta}_0 \approx 0$). Simplified analytical formulations described in the companion paper by Stewart et al. are used to predict inertial interaction effects. The predictions are found to be reasonably accurate relative to empirical results, with some limitations for deeply embedded and long-period structures. A collective examination of the empirical and predicted results reveals a pronounced influence of structure-to-soil stiffness ratio on inertial interaction, as well as secondary influences from structure aspect ratio and foundation embedment, type, shape, and flexibility.

INTRODUCTION

Documentation of seismic case history data is a critically important step toward understanding and reliably characterizing complex problems in geotechnical earthquake engineering. In the case of soil-structure interaction (SSI), few empirical studies have been performed due to the limited availability of strong motion data from sites with instrumented structures and free-field accelerographs. In contrast, analytical formulations for SSI are numerous, ranging from complex, three-dimensional finite-element analysis procedures capable of incorporating fully nonlinear dynamic soil modeling [e.g., Borja (1992)] to simplified substructure techniques suitable for implementation in building codes [e.g., Veletsos and Nair (1975)]. While some sophisticated analytical models have been verified using recorded data from nuclear reactor structures or scaled models thereof [e.g., Valera et al. (1977) and Bechtel Power Corporation (1991)], empirical studies incorporating a large number of building sites with strong motion recordings are lacking.

The objectives of this study are to analyze and interpret available earthquake strong motion data to evaluate the effects of inertial interaction on structural response for a range of geotechnical and structural conditions. The results are used to verify simplified inertial interaction analysis procedures modified from Veletsos and Nair (1975) and Bielak (1975). Kinematic interaction, which modifies foundation-level motions relative to free-field motions, is a second-order effect for many buildings and is not the primary subject of this paper.

A companion paper (Stewart et al. 1999) describes (1) simplified procedures for estimating period lengthening ratios and foundation damping factors; and (2) system identification procedures for evaluating modal vibration parameters for various cases of base fixity. In this paper, these procedures are applied for 57 sites in California and Taiwan with strong motion recordings to elucidate the effects of inertial SSI on seismic structural response and to verify the simplified analytical procedures.

SITE SELECTION

Two classes of sites are used in this study: Class A sites, which have a free-field accelerograph and a structure instrumented to record base and roof translations (and in some cases, base rocking as well), and Class B sites, which have structures instrumented to record base rocking as well as base and roof translations but have no free-field accelerographs. This section presents criteria employed for the selection of A sites. The B sites are simply those with the stated structural instrumentation.

Each A site was reviewed for the following: (1) The free-field instrument is not so close to the structure as to be significantly affected by structural vibrations; and (2) the free-field instrument is not so far from the structure that free-field and foundation-level motions exhibit significant incoherence. The procedures by which these checks are made are described in Stewart et al. (1998) and are summarized as follows:

- The check for contamination of free-field motion by structural vibrations is made by examining power spectral density and coherency functions for the free-field and foundation motions. High coherencies between the two motions at modal frequencies, or spectral peaks in free-field motions at modal frequencies, indicate potential contamination. At two of the sites considered in this study (A26 and A29), free-field motions appear to have been contaminated by structural vibrations. In both cases, the structures affecting the free-field motions are not the instrumented structure, and the frequencies at which the contamination occurred are not near the lower-mode frequencies of the instrumented structure. Hence, the data from these sites are retained.
- The incoherence between foundation-level and free-field motions is assumed to follow the empirical models developed using data from the Lotung, Taiwan, LSST array (Abrahamson et al. 1991) and SMART1 array (Abrahamson 1988). Based on these models and a minimum acceptable coherency of 0.8, free-field/structure separations

[1]Asst. Prof., Dept. of Civ. and Envir. Engrg., Univ. of California, Los Angeles, CA 90095.
[2]Prof., Dept. of Civ. and Envir. Engrg., Univ. of California, Berkeley, CA 94720.
[3]Prof., Dept. of Civ. and Envir. Engrg., Univ. of California, Berkeley, CA 94720.

Note. Discussion open until June 1, 1999. Separate discussions should be submitted for the individual papers in this symposium. To extend the closing date one month, a written request must be filed with the ASCE Manager of Journals. The manuscript for this paper was submitted for review and possible publication on August 29, 1997. This paper is part of the ***Journal of Geotechnical and Geoenvironmental Engineering***, Vol. 125, No. 1, January, 1999. ©ASCE, ISSN 1090-0241/99/0001-0038–0048/$8.00 + $.50 per page. Paper No. 16526.

are required to be ≤800 m for 1 Hz structures, 450 m for 2 Hz structures, and 150 m for 4 Hz structures. Free-field/structure pairs with greater separations are not considered. Coherency functions for sites meeting these criteria are generally acceptable. System identification results for a few sites with low coherency are either not used or are assigned a low confidence level designation (Stewart et al. 1999).

Suitable free-field instruments were sought for virtually all instrumented structures in California, and 44 were found (plus one additional structure in Taiwan). An additional 13 structures in California were considered in this study as B sites.

SITE AND STRUCTURE CONDITIONS

The 44 A and 13 B sites considered in this study are listed in Table 1. For the 57 sites, 74 processed data sets are available as a result of multiple earthquake recordings at 13 sites. Fifteen California earthquakes contributed data to this study, the most significant of which are the M_w = 6.0 Whittier, M_w = 6.9 Loma Prieta, M_w = 5.6 Upland, M_w = 7.0 Petrolia, M_w = 7.3 Landers, and M_w = 6.7 Northridge earthquakes. The maximum horizontal accelerations (MHAs) occurring at the sites during these earthquakes are >0.6g, 1 data set; 0.4–0.6g, 3 data sets; 0.2–0.4g, 20 data sets; 0.1–0.2g, 17 data sets; and <0.1g, 33 data sets. Hence, moderate- and low-level shaking is well represented in the database, but data for intense shaking (MHA > 0.4g) are relatively sparse (only four data sets).

There are 45 soil sites and 12 rock sites. The shear-wave velocities V_S indicated in the table are the ratio of effective profile depth to the strain-compatible shear-wave travel time through the profile, as defined in Stewart et al. (1999). Site specific small-strain shear-wave velocity profiles for the sites are given in Stewart and Stewart (1997), although supplemental data have been obtained for several sites since that publication.

The foundation conditions at the sites include 23 buildings with piles or piers and 34 with footings, mats, or grade beams. Most buildings are not embedded (36) or have shallow single-level basements (14). Only seven buildings have multilevel basements. The building heights are broken down as follows: 1–4 stories, 17; 5–11 stories, 27; and >11 stories, 13. The principle lateral force resisting systems are masonry/concrete shear walls, 19; dual wall/frame systems, 11; concrete frames, 4; steel frame, 19; and base isolated, 4.

Site A3 is not listed in Table 1 because the structural instrumentation is only sufficient for evaluations of kinematic interaction. Sites A19 and B8 are omitted from the compilation. Data for Site A19 did not become available by the time this paper was prepared, and there are flaws in the analytical results for Site B8 that cannot be resolved.

EMPIRICAL EVALUATION OF INTERACTION EFFECTS

Comparison of Free-Field and Foundation-Level Structural Motions

A simple investigation of kinematic and inertial interaction effects can be made by comparing indices of free-field and foundation motions. Fig. 1 shows peak horizontal accelerations and 5% damped spectral accelerations at the flexible-base period of the structure $\tilde{T}$ for free-field and foundation-level motions at A sites. The $\tilde{T}$ values were established from system identification analyses. Second-order polynomials are fit to the data in Fig. 1 using linear regression.

The data in Fig. 1 indicate that peak foundation-level acceleration are deamplified relative to the free-field, especially in embedded structures. Earlier studies utilizing smaller databases had similar findings [e.g., Poland et al. (1993)]. Conversely, spectral accelerations at $\tilde{T}$ for foundation motions are generally negligibly deamplified for surface foundations (open circles in Fig. 1), and only modestly deamplified for embedded foundations (solid circles in Fig. 1). These different deamplification levels at different spectral periods can be attributed to frequency dependent kinematic deamplification effects that are maximized at low periods (i.e., T = 0), coupled with potential contributions of inertial interaction to foundation motions for periods near $\tilde{T}$. As it is the spectral acceleration at $\tilde{T}$ that best describes the ground motion controlling structural response, for design purposes, there appears to be little useful ground motion deamplification on surface foundations relative to the free-field and only modest deamplification on most embedded foundations (average reduction of 20%). However, as indicated in Fig. 1(b), significant reductions on the order of 40% can occur in individual cases (typically deeply embedded foundations).

Although significant further study is needed to more fully evaluate kinematic interaction effects, the data in Fig. 1 suggest that for purposes of engineering design, free-field and foundation-level motions are often comparable in amplitude. Hence, a more significant SSI effect would appear to be the modification of structural response associated with the flexibility of foundation support. These inertial interaction effects are examined in the remainder of this paper through evaluations of period lengthening ratios and foundation damping factors.

Period Lengthening and Foundation Damping

System identification analyses were performed for the 57 sites considered in this study using procedures outlined in Stewart et al. (1999). Model vibration periods and damping ratios were evaluated for the fixed-base (T, ζ) and flexible-base ($\tilde{T}$, $\tilde{\zeta}$) cases, respectively. These parameters are listed in Table 1, along with the calculated period lengthening ratio $\tilde{T}/T$, foundation damping factor $\tilde{\zeta}_0 = \tilde{\zeta} - \zeta/(\tilde{T}/T)^3$, and dimensionless structure-to-soil stiffness ratio $1/\sigma = h/(V_S \cdot T)$, where h = effective structure height and V_S = effective soil shear-wave velocity. As described in the companion paper, each site was assigned a confidence level based on the quality of available geotechnical data and the accuracy/uncertainty associated with the identification. These confidence levels are indicated in Table 1, with ''A'' indicating acceptable confidence, ''L'' indicating low confidence, and ''U'' indicating unacceptable confidence. As indicated in the companion paper, unacceptable confidence is associated with one of the following situations:

- U1: Reliable flexible-base parameters could not be developed due to significant incoherence between foundation and free-field motions.
- U2: The structure was so stiff that the roof and foundation level motions were essentially identical, and hence the response could not be established by system identification.
- U3: Fixed-base (A sites) or flexible-base (B sites) parameters could neither be estimated nor obtained directly from system identification.
- U4: Reliable parametric models of structural response could not be developed for unknown reasons.

Presented in Fig. 2 are the variations of $\tilde{T}/T$ and $\tilde{\zeta}_0$ with $1/\sigma$ for sites where there is an ''acceptable'' or ''low'' confidence level in the modal parameters. Also shown are second-order polynomials fit to the acceptable confidence data by regression analysis and analytical results by Veletsos and Nair (1975) for h/r = 1 and 2. Both $\tilde{T}/T$ and $\tilde{\zeta}_0$ are seen to increase

TABLE 1. Compilation of First-Mode Parameters for A and B Sites

Site	Station	Eqk.	MHA (g)	h (ft)	e (ft)	Vs (fps)	β(%)	Transverse									Longitudinal									Conf.
								r_u (ft.)	r_θ (ft.)	$\bar{T}$ (sec.)	T (sec.)	$\bar{\zeta}$ (%)	ζ (%)	$\frac{1}{\sigma}$	$\bar{T}/T$	$\bar{\zeta}_0$	r_u (ft.)	r_θ (ft.)	$\bar{T}$ (sec.)	T (sec.)	$\bar{\zeta}$ (%)	ζ (%)	$\frac{1}{\sigma}$	$\bar{T}/T$	$\bar{\zeta}_0$	
'A' Sites																										
1	Eureka Apts.	PT	0.18	31	0	701	5.1	57	42	0.24	0.15	19.6	15.9	0.29	1.57	15.4	57	77	0.25	0.22	12.8	5.5	0.20	1.09	8.6	A
2	Fortuna Market	PT	0.12	22	0	772	5.6	115	112	0.37	0.36	34.0	26.0	0.08	1.04	11.2	115	122	0.31	0.29	39.4	18.0	0.10	1.08	25.1	L
		PTA	0.19			786	5.8			0.35	0.34	17.2	15.0	0.08	1.05	4.1			0.29	0.28	25.6	17.6	0.10	1.03	9.6	L
4	Emeryville PPP	LP	0.25	218	0	448	6.8	87	94	2.50	2.45	13.0	7.4	0.20	1.02	6.1	87	94	2.58	2.65	12.8	5.9	0.18	1.00	6.9	A
5	Hayward City Hall	LP	0.05	84	0	2210	0.8	66	54	1.16	1.11	3.8	3.5	0.03	1.04	0.7	66	82	0.87	0.85	3.2	4.2	0.04	1.03	0.0	A
6	Hayward 13-St.	LP	0.09	141	0			63	64	U3	U3	U3	U3	U3	U3	U3	63	64	U3	U3	U3	U3	U3	U3	U3	
7	Hollister 1-St.	LP	0.36	30	0	502	7.7	97	75	0.73	0.71	26.9	19.0	0.08	1.03	9.3	97	130	U2	U2	U2	U2	U2	U2	U2	A
8	Piedmont Jr. HS	LP	0.08	25	0	1820	1.3	52	46	0.18	0.16	4.8	2.2	0.09	1.16	3.4	52	59	0.17	0.17	7.0	5.1	0.08	1.00	2.0	A
9	PVPP	CGA	0.21	48	32	970	3.2	53	37	0.53	0.53	8.2	5.2	0.09	1.00	3.0	53	77	U2	U2	U2	U2	U2	U2	U2	L
10	Richmond CH	LP	0.13	33	10	768	3.7	75	54	0.30	0.28	9.2	3.9	0.16	1.08	6.1	75	106	0.27	0.26	14.4	1.4	0.16	1.03	13.1	A
11	San Jose 3-St.	LP	0.27	35	0	2642	0.9	86	68	0.64	0.67	20.6	24.8	0.02	1.00	0.0	86	111	0.60	0.66	20.3	23.6	0.02	1.00	0.0	A
12	El Centro Bldg.	IMP	0.24	54	0	464	6.6	61	55	0.74	0.50	16.0	23.4	0.23	1.47	8.8	61	69	1.23	1.25	33.9	36.6	0.09	1.00	0.0	A
13	Indio 4-St.	LD	0.09	56	15.5	695	4.1	69	58	0.71	0.67	10.3	7.5	0.12	1.05	3.8	69	85	0.66	0.64	10.9	10.9	0.13	1.03	1.0	A
14	Lancaster 3-St.	WT	0.07	26	0	908	2.1	54	47	0.20	0.20	13.4	12.4	0.14	1.00	1.1	54	63	U2	U2	U2	U2	U2	U2	U2	A
15	Lancaster 5-St.	NR	0.07	40	0	1001	2.5	99	83	0.73	0.69	10.0	7.5	0.06	1.06	3.6	99	121	0.72	0.71	8.2	9.1	0.06	1.02	0.0	A
16	Lancaster Airfield	NR	0.08	45	6	953	1.7	11.9	11.9	0.34	0.27	9.9	24.5	0.18	1.28	0.0	11.9	11.9	0.33	0.24	8.9	13.6	0.20	1.34	3.3	L
17	Loma Linda VA	NR	0.06	50	0	1415	3.4	246	248	0.29	0.25	15.0	5.8	0.14	1.17	11.3	246	250	0.32	0.29	10.1	5.6	0.12	1.09	5.7	A
18	Long Beach 7-St.	WT	0.07	58	0	615	3.5	49	46	U3	U3	U3	U3	U3	U3	U3	49	53	1.12	1.14	5.5	6.5	0.08	1.00	0.0	A
20	Long Beach VA	NR	0.07	98	23	1143	2.9	84	83	0.58	0.51	3.1	4.6	0.17	1.13	0.0	84	87	0.58	0.55	4.5	4.1	0.16	1.05	1.0	A
21	LA 2-St. FCCB	SM	0.11	22	0	1006	1.3	71	59	0.79	0.79	9.4	13.3	0.03	1.01	0.0	71	88	0.79	0.82	21.5	17.7	0.03	1.00	3.9	L
		LD	0.05			1010	1.2			0.97	0.98	14.2	14.9	0.02	1.00	0.0			0.90	0.90	18.4	18.9	0.02	1.00	0.0	L
		NR	0.32			981	1.7			0.92	0.95	34.4	40.1	0.02	1.00	0.0			0.83	0.84	33.4	39.5	0.03	1.00	0.0	L
22	LA 3-St. Bldg.	NR	0.28	46	22.5	980	5.9	130	128	U1	U1	U1	U1	U1	U1	U1	130	134	U1	U1	U1	U1	U1	U1	U1	L
23	LA 6-St. Bldg.	NR	0.25	56	14	630	5.2	21.4	20.6	0.89	0.82	5.5	6.9	0.11	1.08	0.0	21.4	22.7	U3	U3	U3	U3	U3	U3	U3	A
24	LA 6-St. Garage	NR	0.22	40	0	870 (tr) 640 (L)	7.3 (tr) 6.2 (L)	159	154	0.52	0.51	6.6	6.1	0.09	1.04	1.1	54	47	0.44	0.28	6.1	6.5	0.23	1.60	4.5	A
25	LA 7-St. Hos.	LD	0.04	68	0	1148	1.2	110	110	1.14	1.18	11.8	12.1	0.05	1.00	0.0	110	110	1.09	1.11	10.1	13.1	0.05	1.00	0.0	A
		NR	0.49			1065	2.5			1.19	1.27	27.1	29.3	0.05	1.00	0.0			1.21	1.19	21.1	28.0	0.05	1.01	0.0	A
26	LA 7-St. Bldg.	NR	0.47	66	13.5	548	7.6	33	30	0.66	0.63	9.2	16.1	0.19	1.04	0.0	33	37	1.04	1.09	7.0	11.5	0.11	1.00	0.0	L
27	LA 15-St. Bldg.	LD	0.03	174	0	1161	1.2	131	110	3.15	3.20	3.9	3.0	0.05	1.00	1.0	131	161	3.09	3.10	2.1	1.8	0.05	1.00	0.3	A
		NR	0.19			1120	2.0			3.12	3.20	8.5	2.8	0.05	1.00	5.6			3.07	3.09	8.8	2.0	0.05	1.00	6.8	A
28	LA 19-St. Bldg.	NR	0.28	220	38	980	5.9	92	76	3.24	3.45	U1	U1	0.07	1.00	U1	92	113	3.72	3.89	U1	U1	0.06	1.00	U1	A
29	LA Hollywood SB	WT	0.21	96	9	930	2.8	59	42	1.80	1.77	9.1	5.4	0.06	1.01	3.9	59	86	U4	U4	U4	U4	U4	U4	U4	L
		NR	0.39			879	4.4			2.10	2.05	18.3	15.4	0.05	1.02	3.9			0.80	0.75	8.0	8.5	0.15	1.06	0.9	L
30	LA Wadsworth	NR	0.25	78	17	981	6.3	189	199	1.00	0.92	9.3	9.3	0.09	1.08	1.9	189	199	U3	U3	U3	U3	U3	U3	U3	A
31	Newport Beach	LD	0.04	94	0	1009	2.3	61	52	0.84	0.70	4.7	2.9	0.13	1.19	3.0	61	74								A
		NR	0.11			969	3.2			0.86	0.75	3.2	8.5	0.13	1.16	0.0			0.77	0.67	3.9	4.4	0.14	1.14	0.9	A
32	Norwalk 12400	WT	0.23	70	13.5	730	6.8	93	83	U3	U3	U3	U3	U3	U3	U3	93	106	1.48	1.54	9.6	8.5	0.06	1.00	1.1	A
33	Norwalk 12440	WT	0.23	72	15	794	7.3	142	105	1.32	1.32	2.0	1.8	0.07	1.00	0.2	142	195	1.20	1.22	3.5	3.0	0.07	1.00	0.5	A
		NR	0.08			906	4.0			1.28	1.30	6.3	4.9	0.06	1.00	1.4			1.20	1.22	4.6	3.4	0.07	1.00	1.2	A
34	Palmdale 4-St.	NR	0.08	24	0	1575	1.7	69	49	0.20	0.12	18.5	24.1	0.12	1.66	13.1	69	100	0.20	0.16	12.4	4.9	0.09	1.22	9.7	A
35	Pomona 2-St.	WT	0.06	28	10.5	1246	1.6	59	57	0.26	0.25	8.7	5.5	0.09	1.02	3.6	59	63	0.27	0.26	5.8	8.6	0.09	1.02	0.0	A
		UP	0.21			1178	3.2			0.29	0.29	9.2	4.9	0.08	1.01	4.4			0.30	0.30	11.2	12.1	0.08	1.00	0.0	A
36	Pomona 6-St.	UP	0.21	53	12.5	1148	3.1	50	43	U1	U1	U1	U1	U1	U1	U1	50	59	U1	U1	U1	U1	U1	U1	U1	L
		LD	0.07			1188	2.2			1.26	1.07	9.3	13.4	0.04	1.17	1.0			1.20	0.87	9.8	9.5	0.05	1.39	6.2	L
37	Rancho Cuc. LJC	RD	0.04	56	14	1172	1.4	120	87	0.60	0.59	4.3	3.7	0.08	1.03	0.9	120	170	0.60	0.60	5.6	4.2	0.08	1.00	1.4	A
		WT	0.06			1157	1.7			0.65	0.63	4.4	5.0	0.08	1.02	0.0			0.66	0.65	8.4	6.1	0.07	1.01	2.5	A
		UP	0.24			1060	4.5			0.76	0.77	4.7	7.8	0.07	1.00	0.0			0.75	0.77	6.0	6.7	0.07	1.00	0.0	A
		LD	0.11			1039	4.4			0.87	0.85	11.2	12.5	0.06	1.01	0.0			0.89	0.87	17.2	17.4	0.06	1.02	0.9	A
		NR	0.07			1114	2.8			0.76	0.75	4.6	6.9	0.07	1.02	0.0			0.81	0.79	7.5	8.9	0.06	1.02	0.0	A
38	San Bern. 3-St.	LD	0.09	29	0	883	3.8	78	77	0.56	0.52	6.2	7.2	0.06	1.07	0.4	78	80	0.57	0.55	7.6	10.9	0.06	1.03	0.0	L
39	San Bern. 5-St.	NR	0.07	52	13	1233	2.6	95	86	0.63	0.65	9.1	5.2	0.06	1.00	3.9	95	107	0.50	0.51	7.5	6.2	0.08	1.00	1.3	L
40	San Bern. 9-St.	LD	0.10	74	0	848	3.4	55	52	2.01	2.01	5.0	6.8	0.04	1.00	0.0	55	59	2.05	2.08	7.4	6.0	0.04	1.00	1.3	A
41	San Bern. CGC	NR	0.04	38	0	1011	2.4	114	114	0.51	0.51	2.6	3.4	0.07	1.01	0.0	114	114	0.93	0.91	4.5	4.0	0.04	1.02	0.7	A
42	Santa Susana	NR	0.28	91	0	4460	1.0	23.5	20.5	0.54	0.53	19.1	15.1	0.04	1.02	4.9	23.5	27.6	0.54	0.55	11.4	8.3	0.04	1.00	3.1	L
43	Seal Beach 8-St.	LD	0.05	83	16	933	2.6	103	90	1.28	1.26	11.5	13.2	0.07	1.02	0.0	103	121	1.16	1.12	13.7	16.2	0.08	1.04	0.0	A
		NR	0.08			911	3.3			1.21	1.18	6.6	7.1	0.08	1.03	0.0			1.09	1.06	9.1	8.7	0.09	1.03	1.1	A
44	Sylmar Hos.	WT	0.05	63	0	1506	1.9	126	132	0.30	0.27	9.1	9.9	0.16	1.10	1.7	126	132	0.29	0.25	9.5	8.6	0.17	1.17	4.1	A
		NR	0.84			1119	9.1			0.38	0.37	18.9	19.4	0.15	1.04	1.7			0.34	0.26	23.4	17.5	0.21	1.29	15.2	A
45	Ventura 12-St.	NR	0.06	69	0	886	2.8	62	47	0.71	0.53	4.0	5.7	0.15	1.34	1.6	62	83								A
46	Lotung Reactor	L07	0.11	47	15	275	9.7	16.3	16.3	0.49	0.12	30.6	3.0	1.45	4.14	30.6	16.3	16.3	0.45	0.11	31.0	3.0	1.54	4.01	31.0	A
'B' Sites																										
1	Milpitas 2-St.	LP	0.14	26	0	649	4.1	6.4	10.9	0.25	0.24	15.3	21.9	0.17	1.06	0.0										A
2	San Bruno 9-St.	LP	0.11	66	0	916	3.6	72	59	1.10	0.97	12.5	11.4	0.07	1.13	4.7										A
3	San Fran. 47-St.	LP	0.16	414	27	478	4.3	86	80	5.16	5.03	U4	U4	0.17	1.03	U4										A
4	San Fran. Trans.	LP	0.12	475	51	801	5.9	98	99	U3	U3	U3	U3	U3	U3	U3										A
5	San Jose 10-St.	LP	0.12	61	0	768	4.1	65	49	0.48	0.29	6.7	18.6	0.27	1.64	2.5										A
6	San Jose 13-St.	LP	0.10	109	13.5	725	3.5	83	84	2.16	2.13	1.0	1.3	0.07	1.01	0.0	83	84	2.19	2.17	2.8	2.2	0.07	1.01	0.6	A
7	Walnut Crk 10-St	LP	0.10	89	14	1405	1.2	32	26	0.77	0.66	6.6	13.3	0.10	1.17	0.0										A
9	El Segundo 14-St.	NR	0.13	114	0	899	4.1	69	64	U3	U3	U3	U3	U3	U3	U3										A
10	LA 9-St.	NR	0.16	89	13	878	3.7	50	38	1.25	1.25	10.3	7.8	0.08	1.00	2.5	65	67	1.06	1.04	11.5	13.0	0.10	1.03	0.0	A
11	LA 17-St.	LD	0.04	91	0	1190	0.9	76	35.2	0.96	0.85	4.1	3.4	0.09	1.13	1.7										A
		NR	0.26			1140	1.4			1.05	0.90	4.9	3.9	0.09	1.17	2.5										A
12	LA 32-St.	NR	0.11	300	54	1339	1.2	93	91	1.94	1.84	7.6	7.1	0.12	1.06	1.7	93	97	U3	U3	U3	U3	U3	U3	U3	A
13	LA 54-St.	NR	0.14	414	57.5	1317	3.4	96	87	5.81	5.70	7.7	15.0	0.06	1.02	0.0										A
14	Whittier 8-St.	NR	0.17	48	0	842	3.2	64	28.5	0.56	0.49	12.1	12.9	0.12	1.14	3.4										A

h= effective structure height ≈ 0.7 · full height
e= embedment depth
Vs= soil shear wave velocity
β = soil hysteretic damping
Vs and β evaluated from soil profiles in Stewart (1997)

U1-U4 denote unacceptably low confidence results that are unreported
A, L denote acceptable and low confidence in results, respectively
blank entries = insuffiencient strong motion data to evaluate modal parameters
r_u, r_θ =foundation radii matching area and moment of inertia of actual foundation
$1/\sigma = h / (V_s \cdot T)$

* Lateral force resisting systems:
SW = shear wall, masonry or conc.
DWF = dual wall/frame system
CF = concrete frame
SF = steel frame
BI = base isolated

Earthquakes: CGA=Coalinga Aftershock, IMP=Imperial Valley, LD=Landers, LP=Loma Prieta, L07=Lotung Event 7, NR=Northridge, PT=Petrolia, PTA=Petrolia Aftershock, RD=Redlands, SM=Sierra Madre, UP=Upland, WT=Whittier

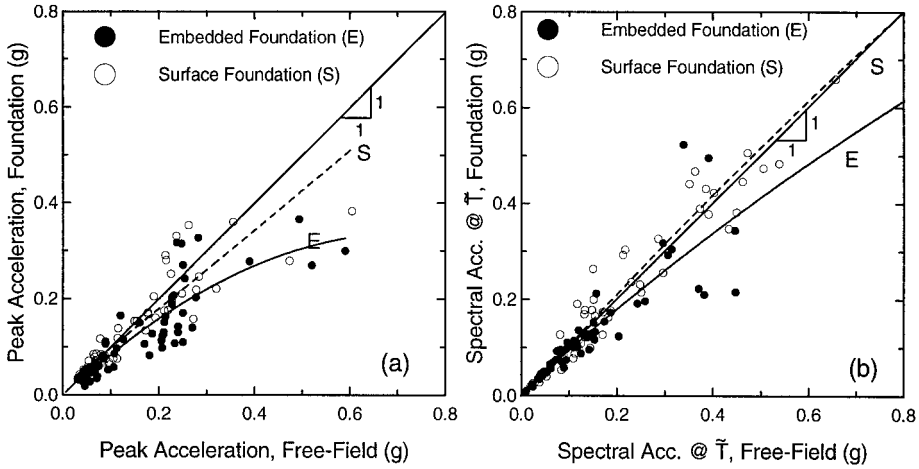

FIG. 1. Comparison of Free-Field and Foundation-Level Structural Motions: (a) Peak Acceleration Data; (b) 5% Damped Spectral Accelerations at $\tilde{T}$

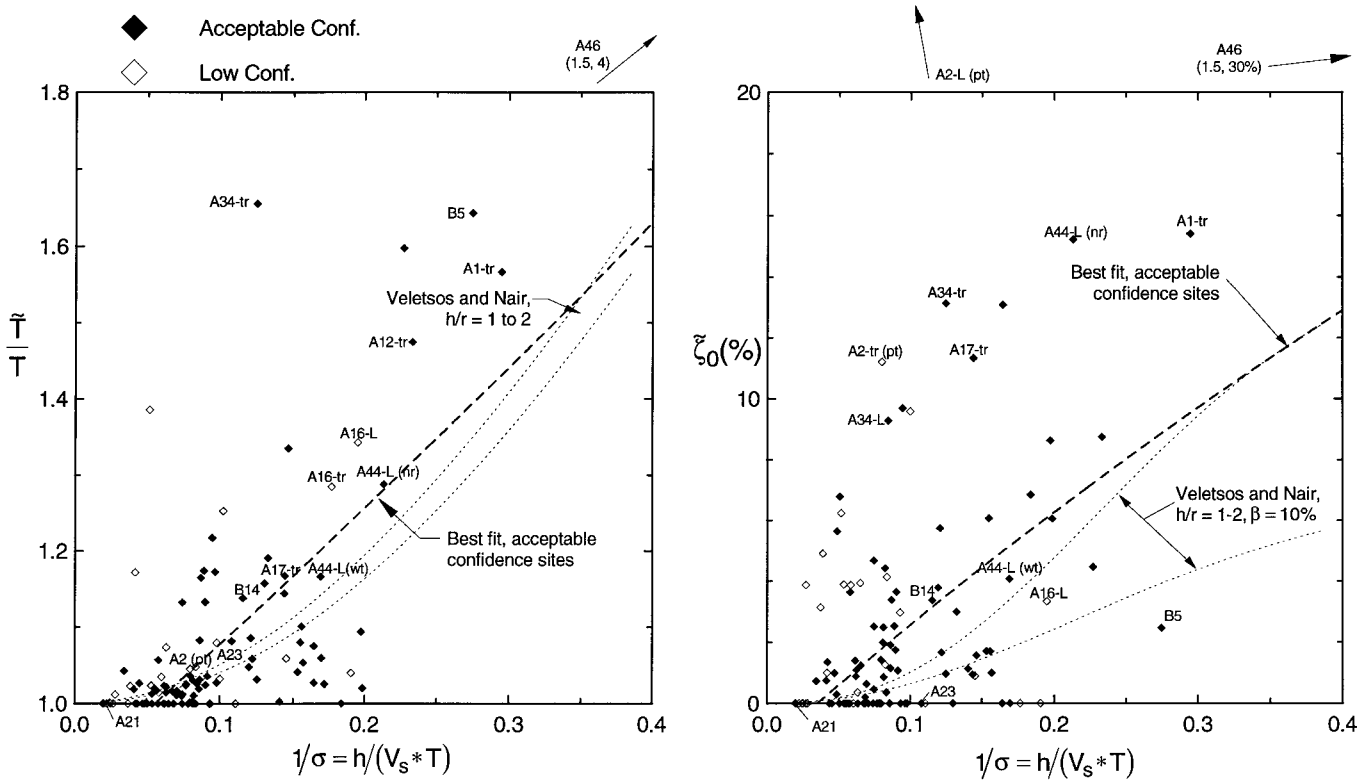

FIG. 2. Period Lengthening Ratio and Foundation Damping Factor for Sites Sorted by Confidence Level and Analytical Results from Veletsos and Nair (1975) (tr = Transverse, L = longitudinal)

with $1/\sigma$, and the best-fit lines through the data are similar to the Veletsos and Nair curves.

There is significant scatter in the data in Fig. 2, although much of this results from systematic variations in $\tilde{T}/T$ and $\tilde{\zeta}_0$ associated with factors such as structure aspect ratio and foundation embedment, type, shape, and flexibility effects. In addition, $\tilde{\zeta}_0$ is influenced by the hysteretic soil damping β, which varies with soil type.

Results from several sites help to illustrate the strong influence of $1/\sigma$ on inertial interaction effects. The most significant inertial interaction occurred at Site A46 ($\tilde{T}/T \approx 4$ and $\tilde{\zeta}_0 \approx 30\%$), which has a stiff ($T \approx 0.1$ s) cylindrical concrete structure (h = 14.3 m, r = 4.9 m) and relatively soft soils ($V_S \approx 85$ m/s), giving a large $1/\sigma$ of $\sim$1.5. Conversely, the inertial interaction effects are negligible at Site A21 ($\tilde{T}/T \approx 1$ and $\tilde{\zeta}_0 \approx 0\%$), which has a relatively flexible ($T \approx 0.8-1.0$ s) base-isolated structure (h = 6.7 m, r_u = 21.6 m) that is founded on rock ($V_S \approx 300$ m/s), giving a much smaller $1/\sigma$ value of 0.02–0.03. These two sites represent the extremes of inertial interaction. More typical SSI effects occur at Sites B14 ($\tilde{T}/T$ = 1.14 and $\tilde{\zeta}_0 \approx 3.4\%$) and A1-tr ($\tilde{T}/T$ = 1.57 and $\tilde{\zeta}_0 \approx 15.4\%$). The structures at both sites are shear wall buildings with periods of T = 0.49 and 0.15 s, respectively, and are founded on medium-stiff soils (V_S = 256 and 213 m/s), combining to give $1/\sigma \approx 0.12$ at Site B14 and $1/\sigma \approx 0.29$ at Site A1-tr. The results from these four sites illustrate that both $\tilde{T}/T$ and $\tilde{\zeta}_0$ increase with increasing $1/\sigma$.

To examine the influence of parameters other than $1/\sigma$ on SSI effects, the data in Fig. 2 were sorted according to aspect ratio h/r_0, foundation type (piles or piers versus shallow foundations), embedment ratio e/r, and lateral force resisting system by Stewart et al. (1998). The trends resulting from these regressions are relatively weak, as the influence of the respective parameters could not be readily isolated from each other

given the limited scope of the database. Nonetheless, some dependence on aspect ratio was found, with larger period lengthening and smaller damping for structures with $h/r_\theta > 1$ than for structures with $h/r_\theta < 1$. This is consistent with trends from the analytical models. Well-defined trends in data sorted according to other parameters were not identified.

CALIBRATION OF SIMPLIFIED ANALYSIS PROCEDURES FOR INERTIAL INTERACTION

Overview of Analysis Procedures

Simplified analyses for inertial interaction estimate the first-mode period lengthening ratio $\tilde{T}/T$ and foundation damping factor $\tilde{\zeta}_0$ given the fixed-base properties of the structure T and ζ and parameters describing foundation and site conditions, as described in the companion paper (Stewart et al. 1999). One methodology is termed the ''modified Veletsos'' (MV) formulation, because it is based on the impedance function in Veletsos and Verbic (1973) and the derivations for $\tilde{T}/T$ and $\tilde{\zeta}_0$ in Veletsos and Nair (1975) for a single-degree-of-freedom structure supported on a rigid circular foundation resting on the surface of a homogeneous viscoelastic half-space. The modified terms refers to adjustments to the impedance function required to account for the effects of nonuniform soil profiles and foundation embedment, shape, and flexibility. Due to shortcomings in the impedance function adjustments for foundation embedment effects, a second analysis procedure adapted from Bielak (1975) is used for embedded structures. This ''modified Bielak'' (MB) procedure utilizes the same impedance function modifiers for nonuniform soil profiles and foundation shape and flexibility effects as are used in the MV approach.

Table 1 presents the input parameters required for these analyses including strain-dependent ''representative'' soil shear-wave velocity V_S and hysteretic damping ratio β, effective height of structure h, foundation embedment e, and foundation radii that match the area A_f and moment of inertia I_f of the actual foundation ($r_u = \sqrt{A_f/\pi}$ and $r_\theta = \sqrt[4]{4I_f/\pi}$). Using these parameters, $\tilde{T}/T$ and $\tilde{\zeta}_0$ were predicted using the MV formulation for each site. For sites with embedded structures, $\tilde{T}/T$ and $\tilde{\zeta}_0$ were also evaluated by the MB formulation. The empirical and predicted values of $\tilde{T}/T$ and $\tilde{\zeta}_0$ are listed in Table 2.

Accuracy of MV Formulation

Deviations in MV predictions of $\tilde{T}/T$ and $\tilde{\zeta}_0$ relative to empirical values are shown in Fig. 3 for sites with acceptable and low confidence designations. Also plotted are best-fit second-order polynomials established from regression analyses on data from acceptable confidence sites. For most sites, the predictions are accurate to within absolute errors of about ± 0.1 in $\tilde{T}/T$ and $\pm 3\%$ damping in $\tilde{\zeta}_0$ for $1/\sigma = 0-0.4$. The regression curves for $\tilde{T}/T$ indicate no significant systematic bias in predictions of either $\tilde{T}/T$ or $\tilde{\zeta}_0$ up to $1/\sigma = 0.4$. However, there is a significant downward trend in the best-fit curve for damping for $1/\sigma > 0.5$ (beyond the range on Fig. 3) due to a large underprediction of $\tilde{\zeta}_0$ at Site A46 ($1/\sigma = 1.5$), which results from a pronounced embedment effect at this site that is not fully captured by the MV formulation.

The results from several sites help illustrate the general findings of Fig. 3. The minimal inertial interaction effects at Site A21 ($1/\sigma = 0.02-0.03$, $\tilde{T}/T \approx 1$ and $\tilde{\zeta}_0 \approx 0\%$) are well predicted by the MV analyses, as is typical for sites with $1/\sigma < 0.1$. The predictions are also generally satisfactory for sites with intermediate $1/\sigma$ values such as Sites B14 and A1-tr ($1/\sigma = 0.12$ and 0.29, respectively). At these sites, period lengthenings of 1.14 and 1.57 are over- and underpredicted by absolute differences of about 0.11 and 0.06, respectively, while foundation damping factors of 3.4 and 15.4% are underpredicted by absolute differences of 2.3 and 4.8%, respectively. The large inertial interaction effects at Site A46 ($1/\sigma = 1.5$, $\tilde{T}/T \approx 4.0$, and $\tilde{\zeta}_0 \approx 30\%$) are predicted to within an absolute difference of ~ 0.4 for period lengthening, but damping is underpredicted by an absolute difference of $\sim 14\%$. With the exception of the damping results at Site A46 (where there is a significant embedment effect), these results indicate that predictions of $\tilde{T}/T$ and $\tilde{\zeta}_0$ by the MV procedure are reasonably good considering the breadth of conditions represented in the database.

There are several noteworthy outliers in Fig. 3. The significance of these outliers is clarified by normalizing the differences between the empirical and predicted SSI effects by the magnitude of the SSI effect. In Fig. 4, errors in period lengthening ratio are normalized by empirical period lengthening, while errors in foundation damping factors are normalized by empirical flexible-base damping (normalization by empirical $\tilde{\zeta}_0$ was not practical, as some values of $\tilde{\zeta}_0$ are nearly zero). Based on Fig. 4, the most significant outliers for period lengthening are seen to be Site A34 and several long period structures (Sites A4 and B3). Long period structures are subsequently discussed. The unusual results at Site A34 may be associated with erroneously high shear-wave velocity measurements (Stewart et al., in press, 1998). The normalization of damping in Fig. 4 produces substantial scatter, with few clear outliers.

Effect of Embedment: Comparison of MV and MB Predictions

Plotted in Fig. 5 are deviations between analytical and empirical results for three data sets: (1) MV predictions for buildings with surface foundations; (2) MV predictions for buildings with embedded foundations; and (3) MB predictions for buildings with embedded foundations. As before, the best-fit curves are second-order polynomials established from regression analyses.

The regression curves in Fig. 5 suggest that $\tilde{T}/T$ is slightly overpredicted for embedded structures (by either MV or MB) and fairly well-predicted for surface structures. For a given structure with foundation embedment, the differences between MV and MB predictions are generally minor (e.g., absolute differences of ~ 0.02 at Site A20-tr and 0.02 at Site A23) for typical values of $1/\sigma$ (i.e., <0.4). At Site A46 ($1/\sigma = 1.5$), the absolute difference between the predictions is ~ 1.2, which is modest compared to the empirical value of $\tilde{T}/T \approx 4.0$.

The accuracy of $\tilde{\zeta}_0$ predictions by the MV methodology are comparable for surface and embedded structures. However, there are disparities between the MB and MV $\tilde{\zeta}_0$ predictions for embedded structures that increase with $1/\sigma$ (e.g., absolute differences of 0.7% at Site A23, $1/\sigma = 0.11$; 2.7% at Site A20-tr, $1/\sigma = 0.17$; 10% at Site A46, $1/\sigma = 1.5$). The regression curves are primarily controlled by the shallowly embedded foundations ($e/r < 0.5$), which are the most numerous in the database. For such cases, MV predictions are typically more accurate than MB predictions, as shown by the regression curves in Fig. 5 and as illustrated by Sites A20 ($e/r = 0.27$) and A26 ($e/r = 0.41$). However, there are systematic errors in MV predictions for more deeply embedded foundations. These errors are not surprising because only the MB formulation incorporates dynamic basement wall/soil interaction effects into the foundation impedance function (Stewart et al. 1999). As shown by individual labeled sites in Fig. 5, MV predictions of $\tilde{\zeta}_0$ are generally too low for relatively deeply embedded structures with continuous basement walls around the building perimeter such as Site A46 ($e/r = 0.92$) as well as Sites A9, B12, and A16-L ($e/r > 0.5$). Other structures in the database

with $e/r > 0.5$ had negligible foundation damping (i.e., $\tilde{\zeta}_0 < 1\%$), which was overestimated by both MV and MB predictions (i.e., Sites A16-tr and B13). Hence, it appears that MB predictions of $\tilde{\zeta}_0$ are generally more accurate than MV predictions for structures with $e/r > 0.5$ and significant SSI effects. These differences are most pronounced at Site A46, where the MB prediction of $\tilde{\zeta}_0 = 27\%$ matches the empirical value of 30% better than the MV prediction of 17%.

In summary, the accuracy of period lengthening predictions by the MV methodology are reasonably good for surface and shallowly embedded structures, and differences between the MV and MB predictions are generally minor for $1/\sigma$ values of common engineering interest ($1/\sigma < 0.4$). Accuracies of MV damping predictions are generally acceptable for surface and shallowly embedded structures ($e/r < 0.5$). For deeper embedment ($e/r > 0.5$), MB damping predictions are generally more

TABLE 2. Inertial Interaction Effects Evaluated from System Identification Analyses and Predicted by MV and MB Formulations

		TRANSVERSE							LONGITUDINAL						
			Observed		Veletsos		Bielak			Observed		Veletsos		Bielak	
Site[a] (1)	Earthquakes (2)	$1/\sigma$ (3)	$\tilde{T}/T$ (4)	$\tilde{\zeta}_0$ (5)	$\tilde{T}/T$ (6)	$\tilde{\zeta}_0$ (7)	$\tilde{T}/T$ (8)	$\tilde{\zeta}_0$ (9)	$1/\sigma$ (10)	$\tilde{T}/T$ (11)	$\tilde{\zeta}_0$ (12)	$\tilde{T}/T$ (13)	$\tilde{\zeta}_0$ (14)	$\tilde{T}/T$ (15)	$\tilde{\zeta}_0$ (16)
(*a*) A sites															
1	PT	0.27	1.57	15.4	1.51	10.6	—	—	0.20	1.09	8.6	1.17	11.6	—	—
2	PT	0.08	1.04	11.2	1.07	4.9	—	—	0.10	1.08	25.1	1.10	7.4	—	—
	PTA	0.09	1.05	4.1	1.07	5.3	—	—	0.10	1.03	9.6	1.11	7.7	—	—
4	LP	0.20	1.02	6.1	1.17	1.7	—	—	0.18	1.00	6.9	1.15	1.4	—	—
5	LP	0.03	1.04	0.7	1.01	0.0	—	—	0.05	1.03	0.0	1.01	0.1	—	—
6	LP	—	U3	U3	—	—	—	—	—	U3	U3	—	—	—	—
7	LP	0.09	1.03	9.3	1.06	3.1	—	—	—	U2	U2	—	—	—	—
8	LP	0.09	1.16	3.4	1.04	1.5	—	—	0.08	1.00	2.0	1.03	1.5	—	—
9	CGA	0.09	1.00	3.0	1.03	1.5	1.03	2.4	—	U2	U2	—	—	—	—
10	LP	0.15	1.08	6.1	1.14	6.3	1.11	12.1	0.17	1.00	13.0	1.12	10.3	1.12	21.3
11	LP	0.02	1.00	0.0	1.00	0.1	—	—	0.02	1.00	0.0	1.00	0.0	—	—
12	IMP	0.19	1.47	8.8	1.26	6.1	—	—	0.10	1.00	0.0	1.03	0.9	—	—
13	LD	0.12	1.05	3.8	1.05	1.6	1.05	2.8	0.12	1.03	1.0	1.04	2.1	1.06	3.4
14	WT	0.14	1.00	1.1	1.11	4.8	—	—	—	U2	U2	—	—	—	—
15	NR	0.06	1.06	3.6	1.02	0.8	—	—	0.06	1.02	0.0	1.02	0.8	—	—
16	NR	0.18	1.28	0.0	1.14	0.2	1.21	1.6	0.17	1.34	3.3	1.17	0.3	1.26	2.1
17	NR	0.14	1.17	11.3	1.21	12.5	—	—	0.12	1.09	5.7	1.15	9.9	—	—
18	WT	—	U3	U3	—	—	—	—	0.08	1.00	0.0	1.02	0.3	—	—
20	NR	0.17	1.13	0.0	1.09	1.6	1.11	4.3	0.16	1.05	1.0	1.08	1.5	1.1	3.8
21	SM	0.03	1.01	0.0	1.01	0.2	—	—	0.03	1.00	3.9	1.00	0.1	—	—
	LD	0.02	1.00	0.0	1	0.1	—	—	0.02	1.00	0.0	1.00	0.1	—	—
	NR	0.02	1.00	0.0	1.01	0.2	—	—	0.03	1.00	0.0	1.01	0.2	—	—
22	NR	0.09	U1	U1	—	—	—	—	0.10	U1	U1	—	—	—	—
23	NR	0.11	1.08	0.0	1.04	0.5	1.06	1.2	—	U3	U3	—	—	—	—
24	NR	0.09	1.04	1.1	1.08	5.1	—	—	0.23	1.60	4.5	1.28	7.2	—	—
25	LD	0.05	1.00	0.0	1.01	0.2	—	—	0.05	1.00	0.0	1.01	0.3	—	—
	NR	0.06	1.00	0.0	1.01	0.3	—	—	0.06	1.01	0.0	1.01	0.3	—	—
26	NR	0.20	1.04	0.0	1.13	2.2	1.16	4.2	0.12	1.00	0.0	1.03	0.6	1.05	1.3
27	LD	0.05	1.00	1.0	1.01	0.1	—	—	0.05	1.00	0.3	1.01	0.1	—	—
	NR	0.05	1.00	5.6	1.01	0.1	—	—	0.05	1.00	6.8	1.01	0.1	—	—
28	NR	0.07	1.00	—	1.02	—	1.02	—	0.06	1.00	—	1.01	—	1.02	—
29	WT	0.06	1.01	3.9	1.03	0.1	1.02	0.1	—	—	—	—	—	—	—
	NR	0.05	1.02	3.9	1.02	0.1	1.01	0.2	0.15	1.06	0.9	1.04	1.4	1.09	1.8
30	NR	0.09	1.08	1.9	1.04	2.1	1.04	3.5	—	U3	U3	—	—	—	—
31	LD	0.13	1.19	3.0	1.11	0.7	—	—	—	—	—	—	—	—	—
	NR	0.13	1.16	0.0	1.11	0.7	—	—	0.14	1.14	0.9	1.06	1.2	—	—
32	WT	—	U3	U3	—	—	—	—	0.06	1.00	1.1	1.01	0.4	1.02	0.6
33	WT	0.07	1.00	0.2	1.03	0.8	1.02	1.4	0.07	1.00	0.5	1.02	1.3	1.03	2.1
	NR	0.06	1.00	1.4	1.02	0.6	1.02	0.9	0.07	1.00	1.2	1.02	0.8	1.02	1.3
34	NR	0.11	1.66	13.1	1.13	5.8	—	—	0.10	1.22	9.7	1.05	3.8	—	—
35	WT	0.09	1.02	3.6	1.04	2.0	1.04	3.2	0.09	1.02	0.0	1.03	1.8	1.04	3.1
	UP	0.08	1.01	4.4	1.03	1.6	1.03	2.6	0.08	1.00	0.0	1.03	1.5	1.03	2.5
36	UP	0.05	U1	U1	—	—	—	—	0.05	U1	U1	—	—	—	—
	LD	0.04	1.17	1.0	1.01	0.1	1.01	0.1	—	1.39	6.2	1.01	0.2	1.01	0.2
37	RD	0.08	1.03	0.9	1.04	1.5	1.03	2.3	0.08	1.00	1.4	1.03	1.7	1.04	2.6
	WT	0.08	1.02	0.0	1.04	1.7	1.03	2.3	0.07	1.01	2.5	1.02	1.4	1.03	2.2
	UP	0.07	1.00	0.0	1.03	0.9	1.02	1.4	0.07	1.00	0.0	1.02	1.2	1.03	1.9
	LD	0.06	1.01	0.0	1.03	2.2	1.02	2.6	0.06	1.02	0.9	1.02	0.9	1.02	1.4
	NR	0.07	1.02	0.0	1.03	0.2	1.02	0.7	0.06	1.02	0.0	1.02	0.9	1.02	1.4
38	LD	0.06	1.07	0.4	1.03	1.2	—	—	0.06	1.03	0.0	1.02	1.1	—	—
39	NR	0.06	1.00	3.9	1.02	0.7	1.02	0.7	0.08	1.00	1.3	1.03	1.4	1.03	2.1
40	LD	0.04	1.00	0.0	1.01	0.1	—	—	0.04	1.00	1.3	1.01	0.1	—	—
41	NR	0.07	1.01	0.0	1.03	1.8	—	—	0.04	1.02	0.7	1.01	0.4	—	—
42	NR	0.07	1.02	4.9	1.02	0.0	—	—	0.07	1.00	3.1	1.01	0.0	—	—
43	LD	0.07	1.02	0.0	1.02	0.3	1.02	0.6	0.08	1.04	0.0	1.02	0.6	1.02	0.9
	NR	0.08	1.03	0.0	1.02	0.4	1.02	0.7	0.08	1.03	1.1	1.02	0.6	1.03	1.0
44	WT	0.16	1.10	1.7	1.12	6.4	—	—	0.17	1.17	4.1	1.14	7.6	—	—
	NR	0.15	1.04	1.7	1.12	6.7	—	—	0.21	1.29	15.2	1.23	12.2	—	—
45	NR	0.15	1.34	1.6	1.14	1.4	—	—	—	—	—	—	—	—	—
46	L07	1.45	4.14	30.6	3.76	17.0	4.94	26.7	1.54	4.01	31.0	3.97	16.9	5.21	26.8

TABLE 2. (*Continued*)

(1)	(2)	(3)	(4)	(5)	(6)	(7)	(8)	(9)	(10)	(11)	(12)	(13)	(14)	(15)	(16)
						(*b*) B sites									
1	LP	0.17	1.06	0.0	1.06	3.4	—	—	—	—	—	—	—	—	—
2	LP	0.08	1.13	4.7	1.17	3.4	—	—	—	—	—	—	—	—	—
3	LP	0.17	1.03	U4	1.20	—	1.24	—	—	—	—	—	—	—	—
4	LP	0.17	U3	U3	—	—	—	—	—	—	—	—	—	—	—
5	LP	0.28	1.64	2.5	1.44	5.2	—	—	—	—	—	—	—	—	—
6	LP	0.07	1.01	0.0	1.02	0.2	1.02	0.3	0.07	1.01	0.6	1.02	0.2	1.02	0.3
7	LP	0.10	1.17	0.0	1.05	0.2	1.05	0.4	—	—	—	—	—	—	—
9	NR	0.06	U3	U3	—	—	—	—	—	—	—	—	—	—	—
10	NR	0.08	1.00	2.5	1.04	0.3	1.03	0.4	0.10	1.03	0.0	1.03	0.5	1.04	0.8
11	LD	0.09	1.13	1.7	1.20	0.2	—	—	—	—	—	—	—	—	—
	NR	0.09	1.17	2.5	1.19	0.3	—	—	—	—	—	—	—	—	—
12	NR	0.12	1.06	1.7	1.05	0.2	1.1	1.0	—	—	—	—	—	—	—
13	NR	0.05	1.02	0.0	1.02	0.1	1.02	0.2	—	—	—	—	—	—	—
14	NR	0.12	1.14	3.4	1.25	1.1	—	—	—	—	—	—	—	—	—

Note: Earthquakes: CGA = Coalinga aftershock, IMP = Imperial Valley, LD = Landers, LP = Loma Prieta, L07 = Lotung event 7, NR = Northridge, PT = Petrolia, PTA = Petrolia aftershock, RD = Redlands, SM = Sierra Madre, UP = Upland, WT = Whittier.
[a]Sites A19 and B8 omitted.

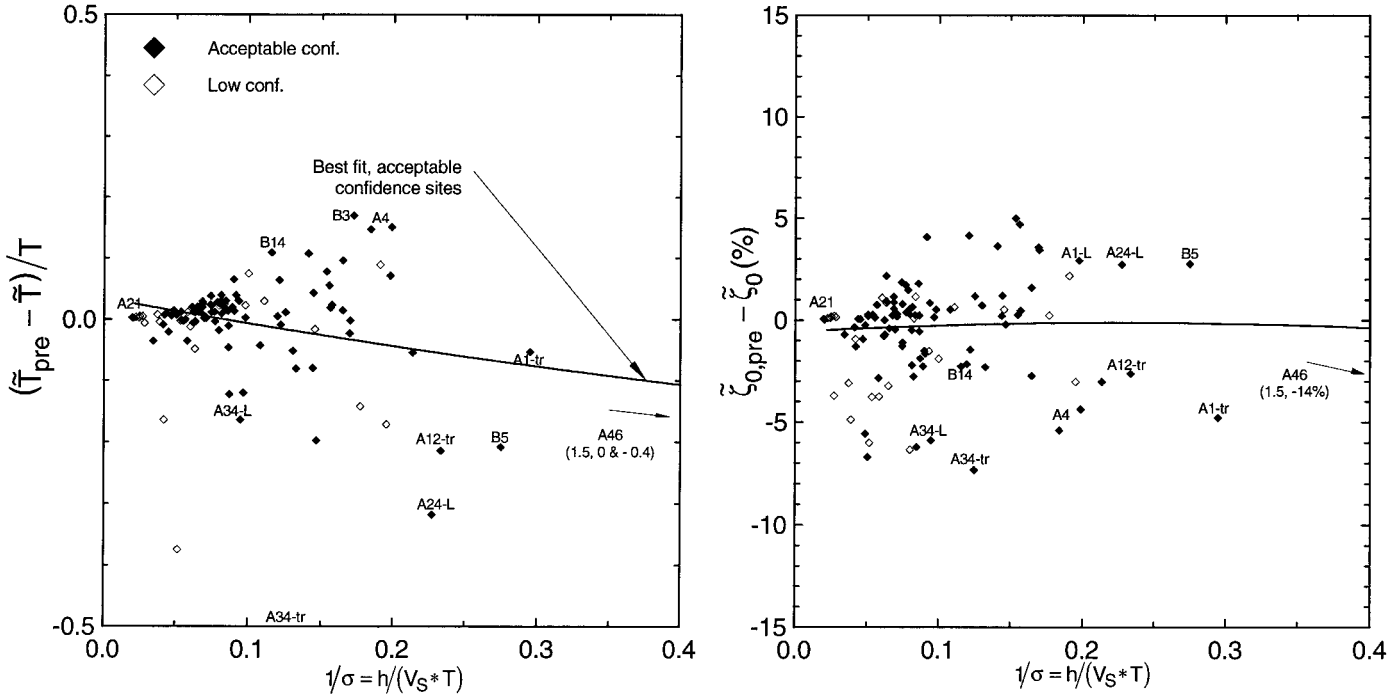

FIG. 3. Errors in MV Formulation for Sites Sorted by Confidence Level (tr = Transverse, L = Longitudinal)

accurate. These results suggest that the dynamic basement-wall/soil interaction modeled by the MB procedure can be important for deeply embedded foundations.

Recognizing the limitations of the MV methodology for high embedment ratios, subsequent plots (Figs. 6 and 7) employ MV predictions for $e/r < 0.5$ and MB predictions for $e/r > 0.5$.

Effects of Aspect Ratio

The results from Fig. 3 (with substitution of MB predictions for $e/r > 0.5$) are replotted in Fig. 6 for aspect ratios of $h/r_\theta < 1$ and $h/r_\theta > 1$. Differences in the average errors of $\tilde{T}/T$ and $\tilde{\zeta}_0$ predictions for structures in both ranges are modest and not statistically significant. Hence, the effects of aspect ratio appear to be reasonably well captured by the analytical formulations.

Effects of Foundation Type

The results from Fig. 3 (with substitution of MB predictions for $e/r > 0.5$) are replotted in Fig. 7 for structures with shallow foundations (i.e., footings, grade beams, and mats) and deep foundations (i.e., piles and piers). Across the range of $1/\sigma$ strongly represented in the database (0–0.2), average errors in predictions of $\tilde{T}/T$ and $\tilde{\zeta}_0$ are comparable for structures with either foundation type, suggesting that the influence of deep foundations on inertial interaction effects is small within this range. However, many of the deep foundation sites for which this trend was established have fairly stiff surficial soils and no marked increase in stiffness across the depth of the foundation elements. For such cases, it is reasonable that dynamic foundation performance would be strongly influenced by the interaction of surface foundation elements (e.g., pile caps, base mats, and footings) with soil. For example, Sites B5 and A24 have 13-m-long friction piles and 5 to 8-m-deep belled piers, respectively, with V_S = 200–300 m/s across the foundation depth (in both cases). Large inertial interaction effects occur at both sites that are slightly underpredicted by the MV procedure, indicating that the deep foundations are unlikely to have contributed significant rocking stiffness or radiation damping to the foundation impedance.

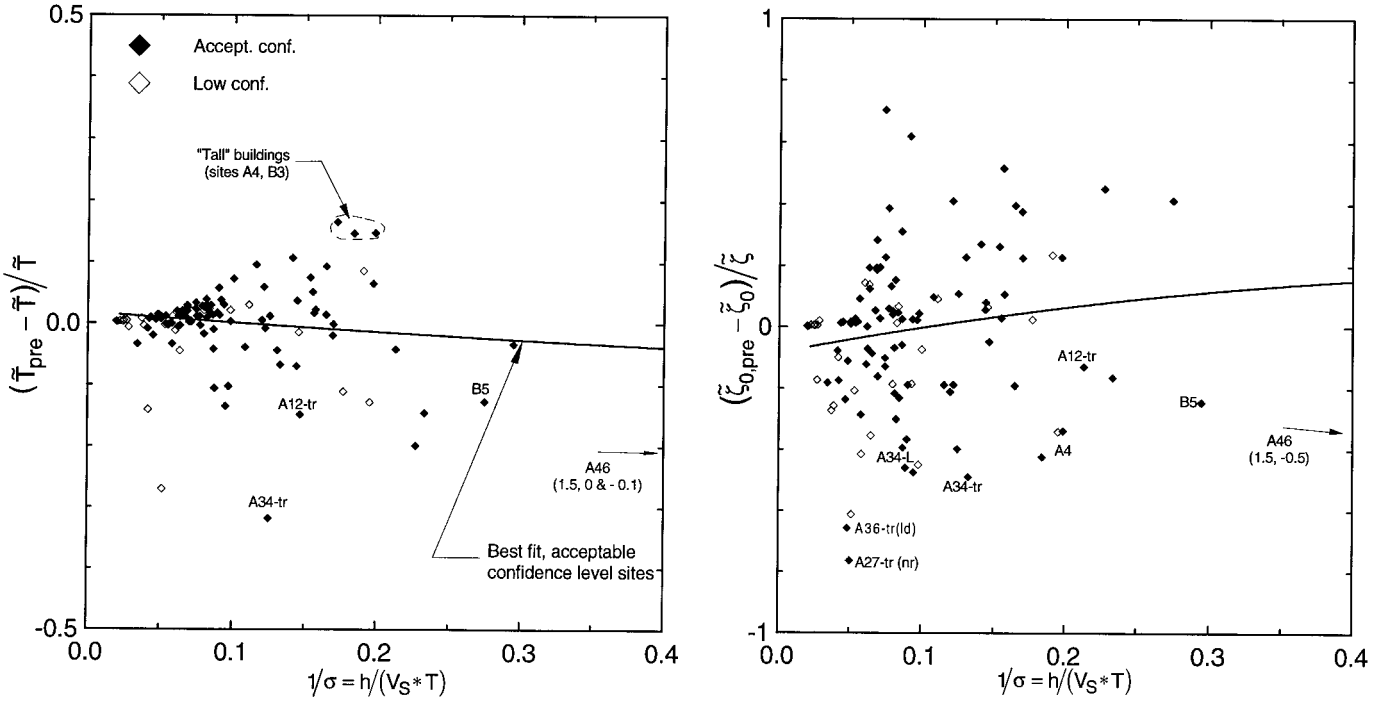

FIG. 4. Errors in MV Formulation for Acceptable and Low Confidence Level Sites with Normalization by Flexible-Base Parameters (tr = Transverse, L = Longitudinal)

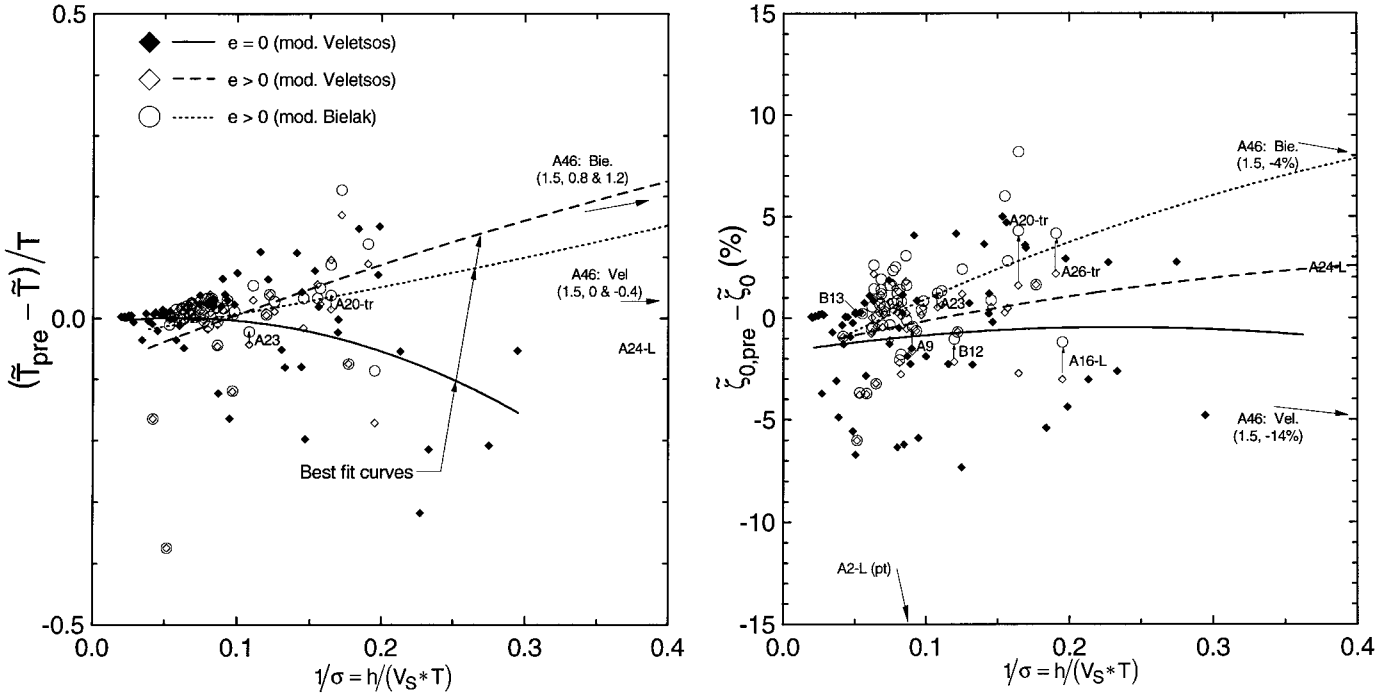

FIG. 5. Errors in MV and MB Formulations for Surface and Embedded Structures (tr = Transverse, L = Longitudinal)

A limited number of sites have foundation piles that pass through relatively soft surficial soils (e.g., V_S < 150 m/s) into stiffer underlying materials (Sites A4, A12, and B3). The period lengthening ratio $\tilde{T}/T$ is overpredicted at Sites A4 and B3, which are pile-supported high-rise structures in the San Francisco Bay area underlain by soft cohesive Holocene sediments. In contrast, period lengthening is underpredicted at Site A12, which is a midheight shear wall structure supported by piles and underlain by soft clays. The contrast in results for these sites suggests that the errors in $\tilde{T}/T$ for these pile supported structures may be associated with factors other than foundation type. With regard to damping, $\tilde{\zeta}_0$ is underestimated at Sites A4 and A12 ($\tilde{\zeta}_0$ not estimated at Site B3), suggesting that soil-pile interaction may have contributed to the foundation damping in these structures.

Effects of Structure Type

Stewart et al. (1998) examined the results in Fig. 3 (with substitution of MB predictions for $e/r > 0.5$) for different types of structural lateral force resisting systems including base-isolated, shear wall, and frame and dual wall/frame buildings. On average, the accuracy of the predictions for these different building types were about the same.

As noted in the previous section and shown in Fig. 3, dif-

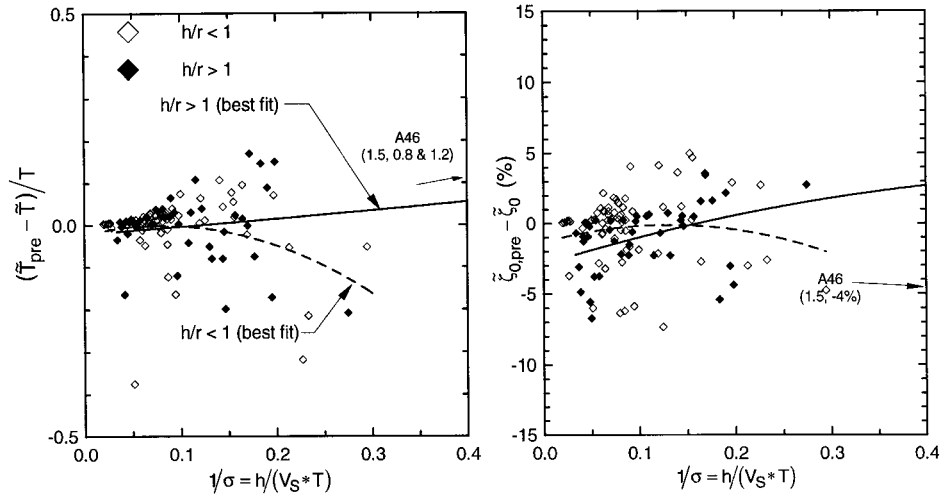

FIG. 6. Errors in Predicted Period Lengthening Ratios and Foundation Damping Factors for Sites Sorted According to Aspect Ratio

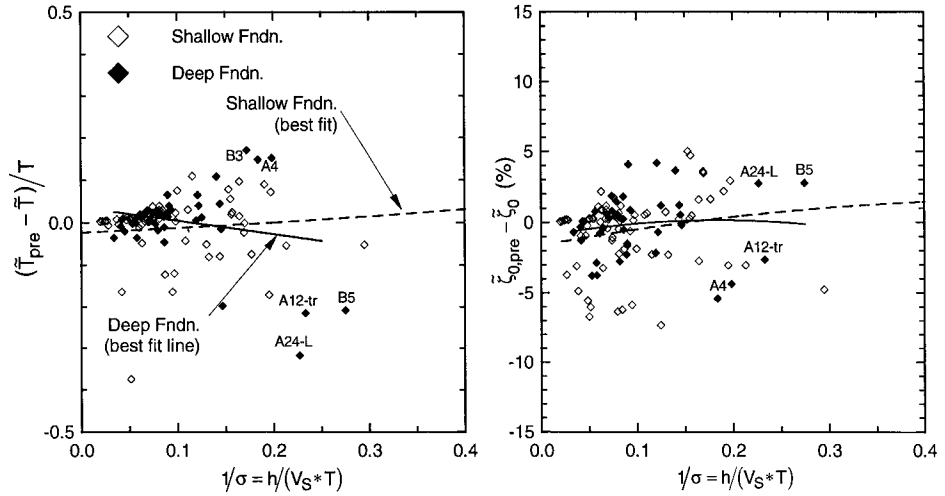

FIG. 7. Errors in Predicted Period Lengthening Ratios and Foundation Damping Factors for Sites Sorted According to Foundation Type (tr = Transverse, L = Longitudinal)

ferences between empirical and predicted inertial interaction effects are significant for two high-rise structures on soft soils (Sites A4 and B3). An examination of system identification results for all the long-period structures ($\tilde{T}$ > 2 s) in Table 1 indicates $\tilde{T}/T$ values near unity. Most of these are founded on relatively stiff soils and have $1/\sigma < 0.06$ [i.e., Sites A27, A28, A29-tr(nr), A40, B6, B9, and B13], so that predictions of $\tilde{T}/T$ are near unity. However, predicted $\tilde{T}/T$ for Sites A4 and B3 are about 1.17–1.24 due to the soft soils and associated large $1/\sigma$ values (0.17–0.20). The cause of the erroneous predictions at these sites may be associated with limitations of the MV and MB single-degree-of-freedom models for structures with significant higher-mode responses.

Effects of Foundation Shape

The evaluation of foundation impedance for both the MV and MB methodologies is based on a circular foundation shape. Different foundation radii are used for translation and rocking deformation modes to match the area and moment of inertia, respectively, of the actual foundation. However, Dobry and Gazetas (1986) found that a noncircular foundation can have a greater radiation damping effect in the rocking mode than a circular foundation with equivalent moment of inertia. Hence, rocking radiation damping values are increased for noncircular foundations according to the criteria in the companion paper (Stewart et al. 1999) in calculating the MV and MB predictions of $\tilde{\zeta}_0$ reported in Table 2. Here we evaluate the significance of shape effects by comparing predicted $\tilde{\zeta}_0$ values developed with and without the corrections to empirical $\tilde{\zeta}_0$ values.

TABLE 3. Empirical and Predicted Values of Foundation Damping Factor $\tilde{\zeta}_0$ Developed with and without Corrections for Shape Effects

Site (1)	Empirical		Predicted	
	S (2)	*S* = 1 (3)	*S* (4)	*S* = 1 (5)
A1-tr	15.4	14.9	10.6	10.3
A10-tr	6.05	5.90	6.33	6.17
A13-L	0.93	0.89	2.11	1.99
A31-L (Northridge)	0.93	0.89	1.15	1.08
A34-tr	12.8	12.0	5.79	5.49
A45-tr	1.55	1.55	1.37	1.31
B2-tr	4.67	4.70	3.40	3.28
B5-tr	2.56	3.14	5.22	4.84

Note: *S* indicates shape correction made; *S* = 1 indicates no correction; tr = transverse direction; L = longitudinal direction.

Shape effect corrections to rocking radiation damping were made in the prediction of $\tilde{\zeta}_0$ values at 31 sites (A1, 5, 7–13, 15, 21, 27–29, 31–34, 36–37, 39, 42–43, 45, B1–2, 5, 7, 10–11, and 14). For 21 sites, the absolute difference in damping associated with the correction is <0.05%. These corrections are small because the radiation damping effect for the rocking deformation mode is small for structures with low fundamental

mode frequencies. For the remaining 10 sites, Table 3 lists empirical $\tilde{\zeta}_0$ values along with predictions made with and without shape effect corrections. The empirical values are dependent on whether the shape effect correction was made because this correction affects fixed- or flexible-base parameters estimated according to the procedures in Stewart and Fenves (1998). The predictions are based on the MV and MB methodologies for $e/r < 0.5$ and $e/r > 0.5$, respectively.

The data in Table 3 indicate no significant improvement in $\tilde{\zeta}_0$ predictions with the shape correction, suggesting that foundation shape effects on rocking radiation damping are minor for the structures in this database.

Effects of Foundation Flexibility

Both the MV and MB methodologies use the assumption of rigid foundations. As discussed in Stewart et al. (1999), foundation flexibility can significantly reduce the rocking stiffness and damping of foundations with continuous base slabs loaded only through rigid central core walls. Three structures in this study have central core shear walls that are designed to resist the bulk of the structure's lateral loads in at least one direction: Sites A24-L, B2, and B7. The foundation for the central core walls at Site B7 is independent of the foundations for the remainder of the structure. Hence, the effects of foundation flexibility are only assessed at Sites A24-L and B2.

The base slab in both of these structures is loaded both through a stiff central core and through vertical load bearing elements outside of the core. Hence, the assumption in the theoretical formulations of a flexible base slab loaded only through a rigid core is not satisfied. The suitability of the theoretical corrections for foundation flexibility [which were adapted from Iguchi and Luco (1982)] are investigated by repeating the predictive analyses for four conditions: (1) Rigid foundation; (2) flexible foundation with corrections to foundation rocking impedance (both stiffness and damping); (3) flexible foundation with corrections to foundation rocking impedance for stiffness only; and (4) rigid foundation beneath central core but perfect flexibility outside of the core (i.e., only the core area is considered in calculating foundation impedance). Shown in Table 4 are the empirical $\tilde{T}/T$ and $\tilde{\zeta}_0$ values along with predictions for the four sets of conditions. At Site B2, it was necessary to estimate flexible-base parameters using procedures in Stewart and Fenves (1998), hence the empirical $\tilde{T}/T$ and $\tilde{\zeta}_0$ values depend on the assumed foundation flexibility. At Site A24, both flexible- and fixed-base parameters are obtained from system identification and hence are unaffected by assumptions about foundation flexibility.

TABLE 4. Comparisons of Empirical Period Lengthening and Foundation Damping for Sites A24-L and B2 with MV Predictions for Different Assumed Conditions of Foundation Flexibility

	A24-L		B2	
Foundation (1)	$\tilde{T}/T$ (2)	$\tilde{\zeta}_0$ (%) (3)	$\tilde{T}/T$ (4)	$\tilde{\zeta}_0$ (%) (5)
Rigid				
Empirical	1.60	4.5	1.19	20.0
Prediction	1.25	13.5	1.03	0.3
Flexible				
Empirical	1.60	4.5	1.13	7.2
Prediction	1.30	13.3	1.17	0.5
Mixed				
Empirical	1.60	4.5	1.13	4.6
Prediction	1.30	14.7	1.17	3.4
Rigid core				
Empirical	1.60	4.5	1.13	5.0
Prediction	1.28	7.2	1.09	0.2

These results indicate that foundation flexibility significantly affects interaction phenomena for these structures. The predictions are poor for the rigid foundation assumption (Condition 1). When corrections to the stiffness and damping components of rocking impedance are made (Condition 2), $\tilde{T}/T$ predictions improve, but $\tilde{\zeta}_0$ predictions are erroneous. For Site A24-L, the best overall results for $\tilde{T}/T$ and $\tilde{\zeta}_0$ are obtained when the foundation area beyond the core is neglected (Condition 4), implying that the pier and grade beam foundation is sufficiently flexible outside of the core and that it does not effectively participate in the structural response of the core. For Site B2, the best results are achieved when corrections for foundation flexibility are only made for stiffness (Condition 3). This result implies that the 0.8–1.5-m-thick foundation slab for this building is unaffected by the vertical load bearing columns outside of the core from the standpoint of rocking stiffness but that the restraint on the foundation provided by these columns effectively eliminates any reduced damping effect that might otherwise result from foundation flexibility.

CONCLUSIONS AND RECOMMENDATIONS

Summary of Findings

Available strong motion data suggest that foundation-level and free-field spectral accelerations at the period of principal interest in structural design (i.e., the first-mode flexible-base period, $\tilde{T}$) are similar for structures with surface foundations and that foundation-level spectral accelerations are generally only modestly deamplified (averaging ~20%) for embedded foundations. Since the free-field and foundation level ground motions therefore appear to be comparable, this study has focused principally on evaluating the effects of inertial interaction on structural response.

Inertial interaction effects for buildings are expressed in terms of the lengthening of first-mode period ($\tilde{T}/T$) and the damping associated with soil-foundation interaction ($\tilde{\zeta}_0$). Simplified analytical procedures for predicting $\tilde{T}/T$ and $\tilde{\zeta}_0$ include MV and MB approaches that are described in the companion paper.

Based on the comprehensive database of 57 sites compiled for this study, the factor with the greatest influence on $\tilde{T}/T$ and $\tilde{\zeta}_0$ is the ratio of structure-to-soil stiffness as quantified by the parameter $1/\sigma = h/(V_S \cdot T)$. When $1/\sigma$ is nearly zero, $\tilde{T}/T$ and $\tilde{\zeta}_0$ values are about unity and zero, respectively, whereas at the maximum observed value of $1/\sigma = 1.5$ at Site A46, interaction effects dominated the structural response ($\tilde{T}/T \approx 4$ and $\tilde{\zeta}_0 \approx 30\%$). Additional factors that can significantly affect inertial interaction include the structure's aspect ratio h/r_θ and foundation embedment and flexibility. For the majority of sites in the database, other factors such as the type of structural lateral force resisting system as well as foundation type and shape, were found to have a relatively small influence on SSI.

Recommendations

Inertial SSI effects can be expressed by a period lengthening ratio $\tilde{T}/T$ and foundation damping factor $\tilde{\zeta}_0$. These factors are used to estimate flexible-base fundamental-mode parameters, which in turn are used in response spectrum based approaches for evaluating base shear forces and deformations in structures (e.g., Fig. 4 in companion paper). A key finding of this research is that these inertial interaction effects can generally be reliably predicted by the MV analysis procedure. However, several caveats apply to this basic recommendation:

1. Inertial interaction effects were generally observed to be small for $1/\sigma < 0.1$ (i.e., $\tilde{T}/T < 1.1$ and $\tilde{\zeta}_0 < 4\%$), and for practical purposes could be neglected in such cases.

2. For structures with foundations having embedment ratios > 0.5, the MB methodology should be used in lieu of MV to appropriately model the extra radiation damping contributed by dynamic soil/basement-wall interaction.
3. Damping results for pile supported structures on soft foundation soils (V_S < 150 m/s) should be interpreted with caution, as the damping is likely to exceed the values predicted from simplified analyses (which assume shallow foundations) due to soil-pile interaction effects.
4. Period lengthening for long-period (T > 2 s) structures with significant higher-mode responses is negligible and can be neglected.
5. Corrections to rocking damping values for foundation shape effects are generally small and can be neglected without introducing significant errors.

ACKNOWLEDGMENTS

Support for this project was provided by the California Department of Transportation, the Earthquake Engineering Research Institute/Federal Emergency Management Agency 1995–1996 NEHRP Fellowship in Earthquake Hazard Reduction, and the U.S. Geological Survey, Department of the Interior (USGS award number 1434-HQ-97-GR-02995). The views and conclusions contained in this document are those of the writers and should not be interpreted as necessarily representing the official policies, either expressed or implied, of the U.S. government.

APPENDIX I. REFERENCES

Abrahamson, N. A. (1988). ''Empirical models of spatial coherency of strong ground motion.'' *Proc., 2nd Workshop on Strong Motion Arrays*, Institute of Earth Sciences, Taipai, Taiwan, 65–92.

Abrahamson, N. A., Schneider, J. F., and Stepp, J. C. (1991). ''Empirical spatial coherency functions for application to soil-structure interaction analyses.'' *Earthquake Spectra*, 7(1), 1–27.

Bechtel Power Corporation. (1991). ''A synthesis of predictions and correlation studies of the Lotung soil-structure interaction experiment.'' *Rep. No. EPRI NP-7307-M*, Electrical Power Research Institute, Palo Alto, Calif.

Bielak, J. (1975). ''Dynamic behavior of structures with embedded foundations.'' *J. Earthquake Engrg. Struct. Dyn.*, 3(3), 259–274.

Borja, R. I., Smith, H. A., Wu, W.-H., and Amies, A. P. (1992). ''A methodology for nonlinear soil-structure interaction effects using time-domain analysis techniques.'' *Rep. No. 101*, Blume Earthquake Engineering Center, Stanford Univ., Stanford, Calif.

Building Seismic Safety Council (BSSC). (1995). ''NEHRP recommended provisions for seismic regulations for new buildings, Part 1, Provisions and Part 2, Commentary.'' *Rep. No. FEMA 222A*, Federal Emergency Management Agency, Washington, D.C.

Dobry, R., and Gazetas, G. (1986). ''Dynamic response of arbitrarily shaped foundations.'' *J. Geotech. Engrg.*, ASCE, 112(2), 109–135.

Iguchi, M., and Luco, J. E. (1982). ''Vibration of flexible plate on viscoelastic medium.'' *J. Engrg. Mech.*, ASCE, 108(6), 1103–1120.

Poland, C. D., Soulages, J. R., Sun, J., and Mejia, L. H. (1993). ''Quantifying the effect of soil-structure interaction for use in building design.'' *Proc., Seminar on Seismological and Engrg. Aspects of Recent Strong Motion Data*, Strong Motion Instrumentation Program, California Division of Mines and Geology, Sacramento, Calif., 43–54.

Stewart, J. P., and Fenves, G. L. (1998). ''System identification for evaluating soil-structure interaction effects in buildings from strong motion recordings.'' *Earthquake Engrg. and Struct. Dyn.*, 27, 869–885.

Stewart, J. P., Fenves, G. L., and Seed, R. B. (1999). ''Seismic soil-structure interaction in buildings. I: Analytical methods.'' *J. Geotech. Engrg.*, ASCE, 125(1), 26–37.

Stewart, J. P., Seed, R. B., and Fenves, G. L. (1998). ''Empirical evaluation of inertial soil-structure interaction effects.'' *Rep. No. PEER-98/07*, Pacific Earthquake Engineering Research Center.

Stewart, J. P., and Stewart, A. F. (1997). ''Analysis of soil-structure interaction effects on building response from earthquake strong motion recordings at 58 sites,'' *Rep No. UCB/EERC 97/01*, Earthquake Engineering Research Center, Univ. of California, Berkeley, Calif., 742.

Valera, J. E., Seed, H. B., Tsai, C. F., and Lysmer, J. (1977). ''Seismic soil-structure interaction effects at Humboldt Bay Power Plant,'' *J. Geotech. Engrg.*, ASCE, 103(10), 1143–1161.

Veletsos, A. S., and Nair, V. V. (1975). ''Seismic interaction of structures on hysteretic foundations.'' *J. Struct. Engrg.*, ASCE, 101(1), 109–129.

Veletsos, A. S., and Verbic, B. (1973). ''Vibration of viscoelastic foundations.'' *J. Earthquake Engrg. Struct. Dyn.*, 2(1), 87–102.

APPENDIX II. NOTATION

The following symbols are used in this paper:

A_f = area of foundation;
e = foundation embedment;
h = effective height of structure (i.e., distance above foundation-level at which building's mass can be concentrated to yield same base moment that would occur in actual structure assuming linear first mode shape);
I_f = moment of inertia of foundation;
r = radius of circular foundation;
r_u, r_θ = radii that match area and moment of inertia, respectively, of assumed circular foundation in impedance function formulations to actual foundation area and moment of inertia;
T, $\tilde{T}$, $\tilde{T}^*$ = fixed-, flexible-, and pseudoflexible-base periods, respectively, for fundamental mode;
V_S = shear-wave velocity of soil;
β = soil hysteretic damping ratio;
ζ, $\tilde{\zeta}$, $\tilde{\zeta}^*$ = fixed-, flexible-, and pseudoflexible-base damping ratios, respectively, for fundamental mode;
$\tilde{\zeta}_0$ = foundation damping factor, defined as $\tilde{\zeta}_0 = \tilde{\zeta} - \zeta/(\tilde{T}/T)^3$; and
σ = ratio of soil-to-structure stiffness, defined as $\sigma = V_S T/h$.